Supplementary Information

Pressure-driven band gap engineering in ion-conducting semiconductor silver orthophosphate

Yang Lu,‡[a] Shengcai Zhu,‡[ab] Eugene Huang,[a] Yu He,[ac] Jiaji Ruan,[a] Gang Liu[a] and Hao Yan*[a]

[a] *Center for High Pressure Science & Technology Advanced Research, Shanghai 201203, China*

[b] *Department of Physics and Astronomy, High Pressure Science and Engineering Center, University of Nevada, Las Vegas, NV 89154, USA*

[c] *Key Laboratory of High-Temperature and High-Pressure Study of the Earth's Interior, Institute of Geochemistry, Chinese Academy of Sciences, Guiyang, Guizhou 550081, China*

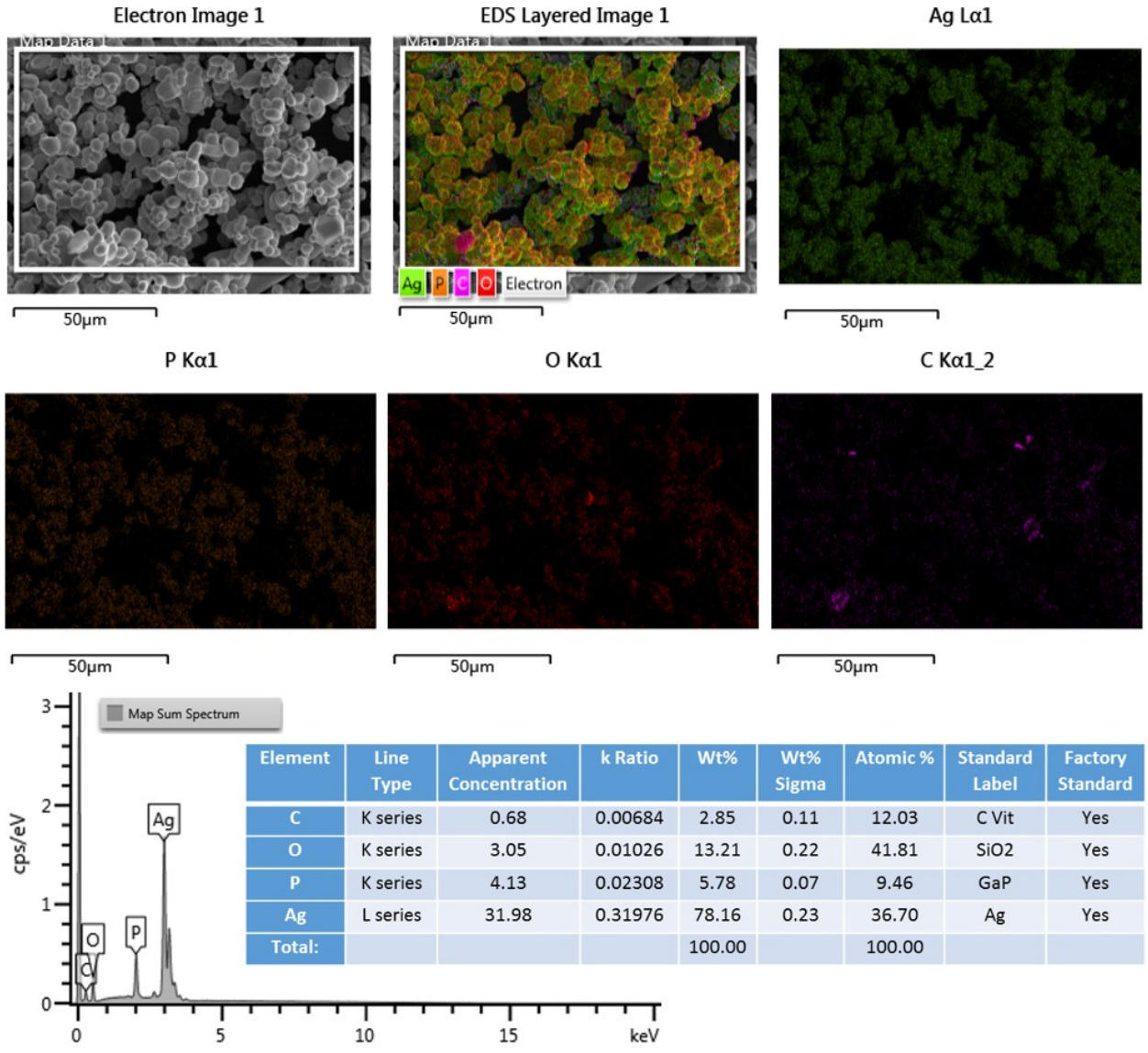

Element	Line Type	Apparent Concentration	k Ratio	Wt%	Wt% Sigma	Atomic %	Standard Label	Factory Standard
C	K series	0.68	0.00684	2.85	0.11	12.03	C Vit	Yes
O	K series	3.05	0.01026	13.21	0.22	41.81	SiO2	Yes
P	K series	4.13	0.02308	5.78	0.07	9.46	GaP	Yes
Ag	L series	31.98	0.31976	78.16	0.23	36.70	Ag	Yes
Total:				100.00		100.00		

Fig. S1 Elements analysis (EDX) of commercial Ag_3PO_4 powder before compression.

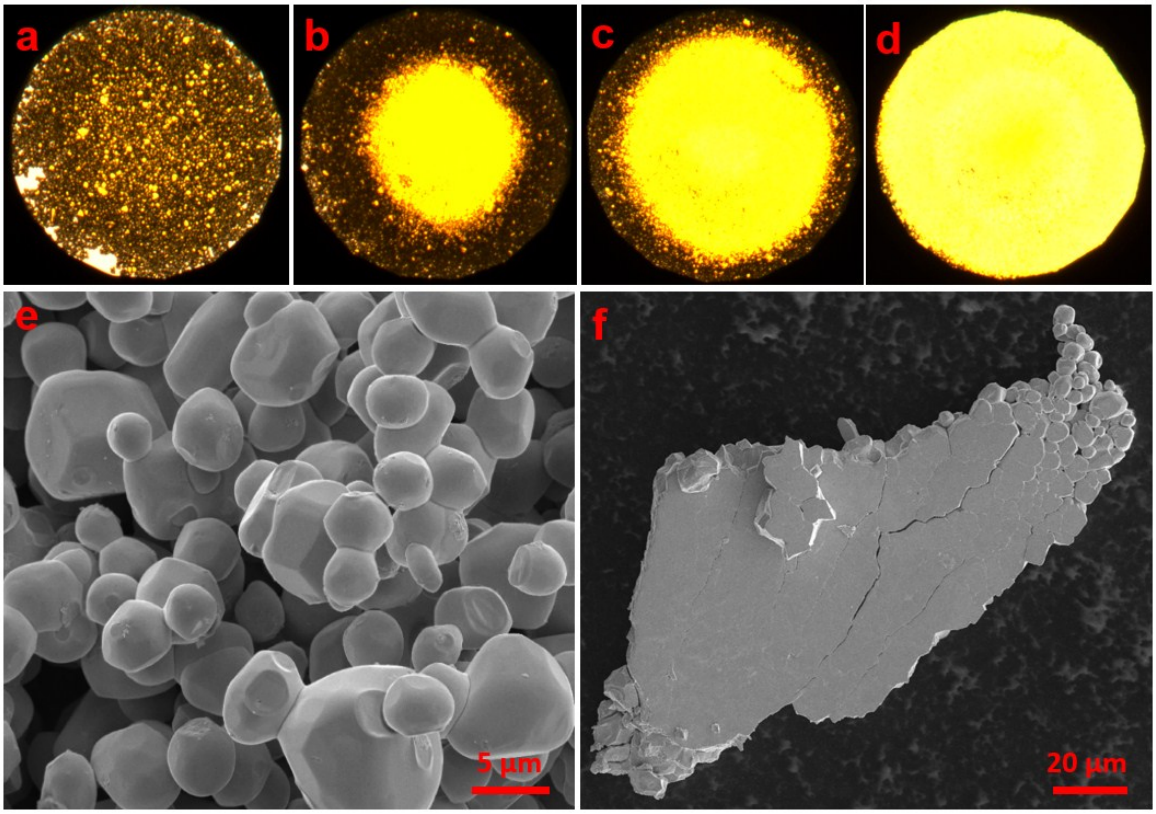

Fig. S2 (a-d) Photographs of the Ag_3PO_4 powder under increasing pressure by diamond anvil cell (500 μm of culets). (e and f) SEM images of the sample before and after compression.

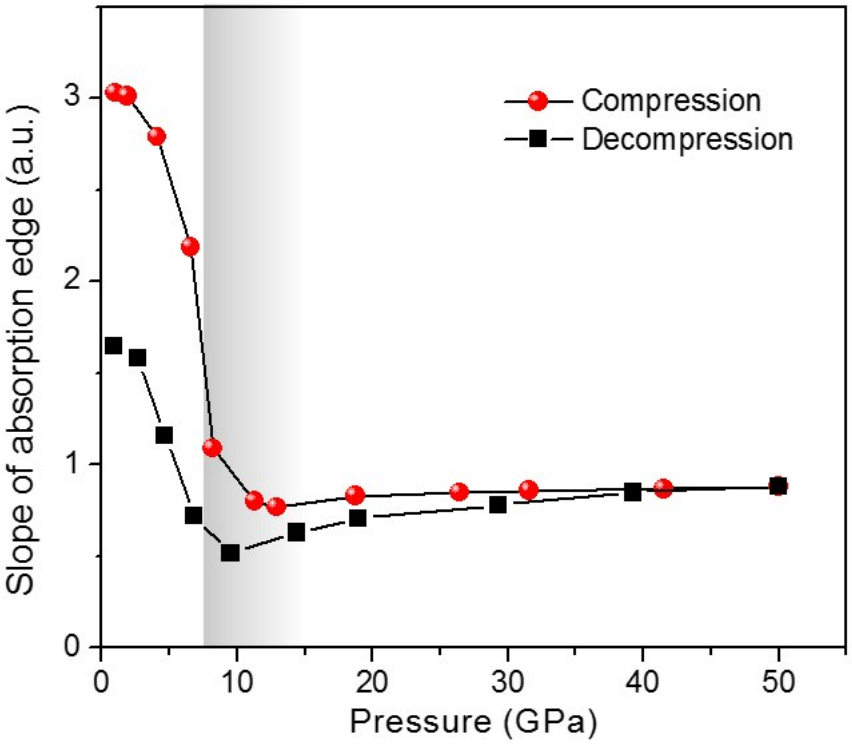

Fig. S3 Pressure-dependent slope of the absorption edge derived from the absorption spectra.

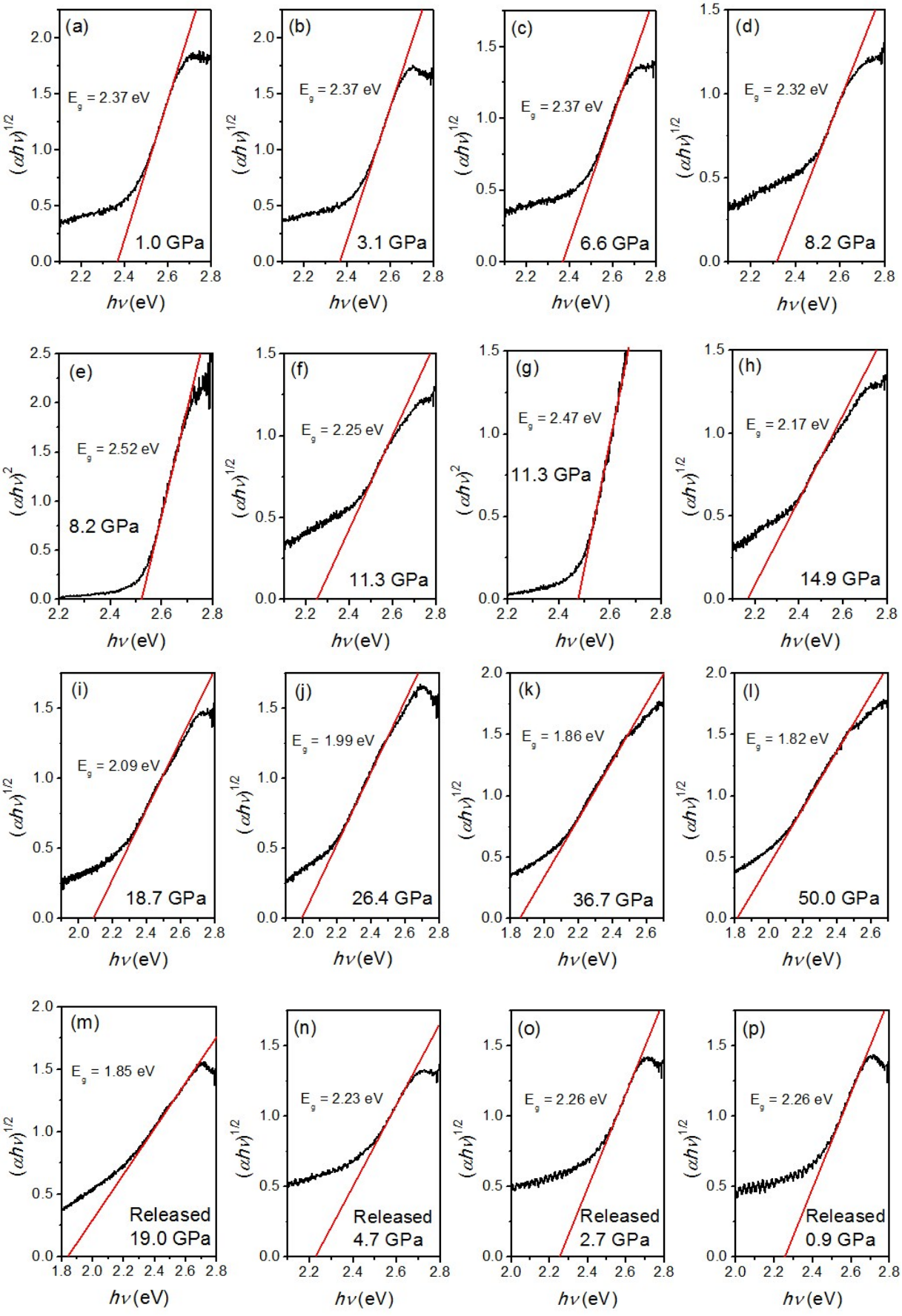

Fig. S4 Tauc plot of the absorbance data and the indirect/direct band gap value of Ag_3PO_4 under pressure.

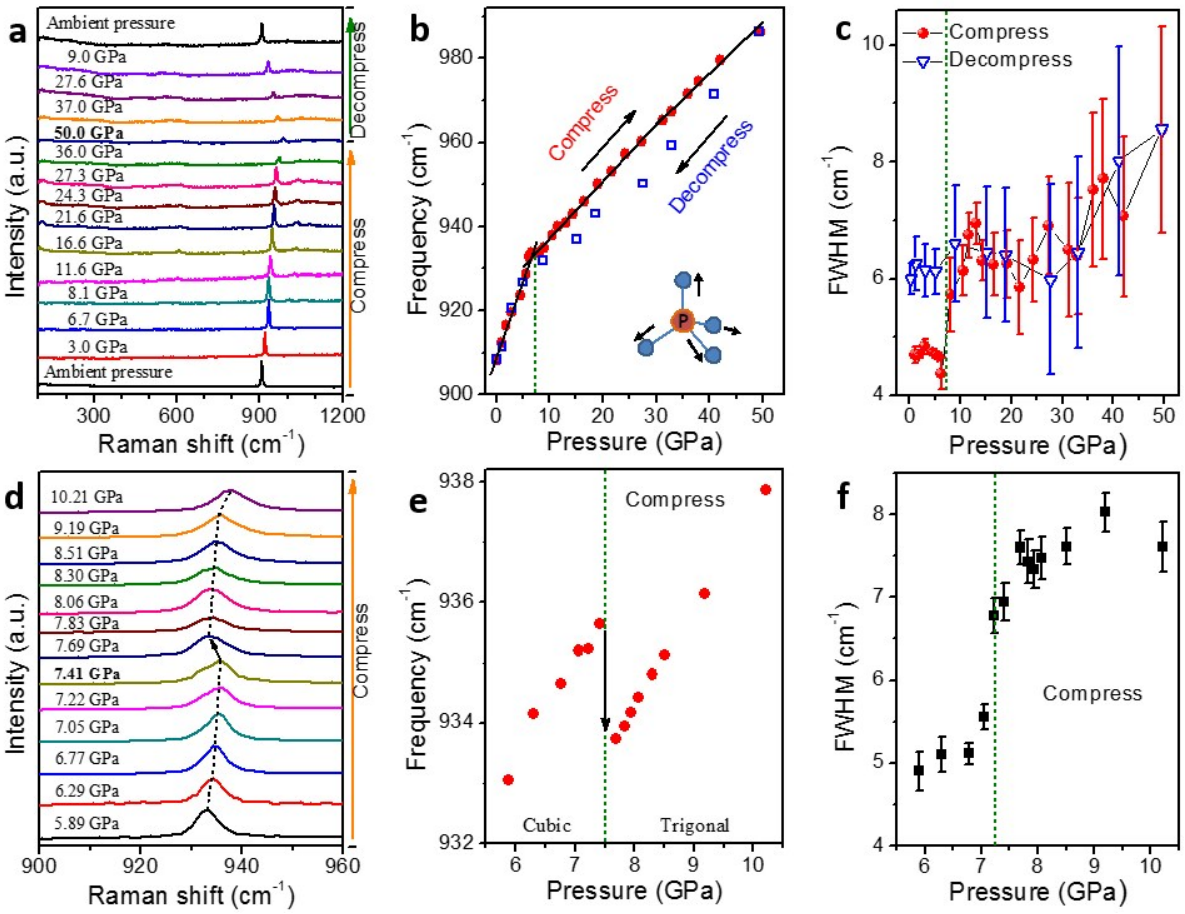

Fig. S5 (a) Selected Raman spectra of Ag_3PO_4 as a function of pressure at room temperature. (b) and (c) Pressure-dependent Raman shift and the full width at half maximum (FWHM) of the prominent peaks at Fig. S5(a), respectively. (d) Raman spectra of the Ag_3PO_4 sample under compression around the phase transition. (e) and (f) The pressure dependence of the frequency and FWHM of the Raman mode derived from Fig. S5(d), respectively.

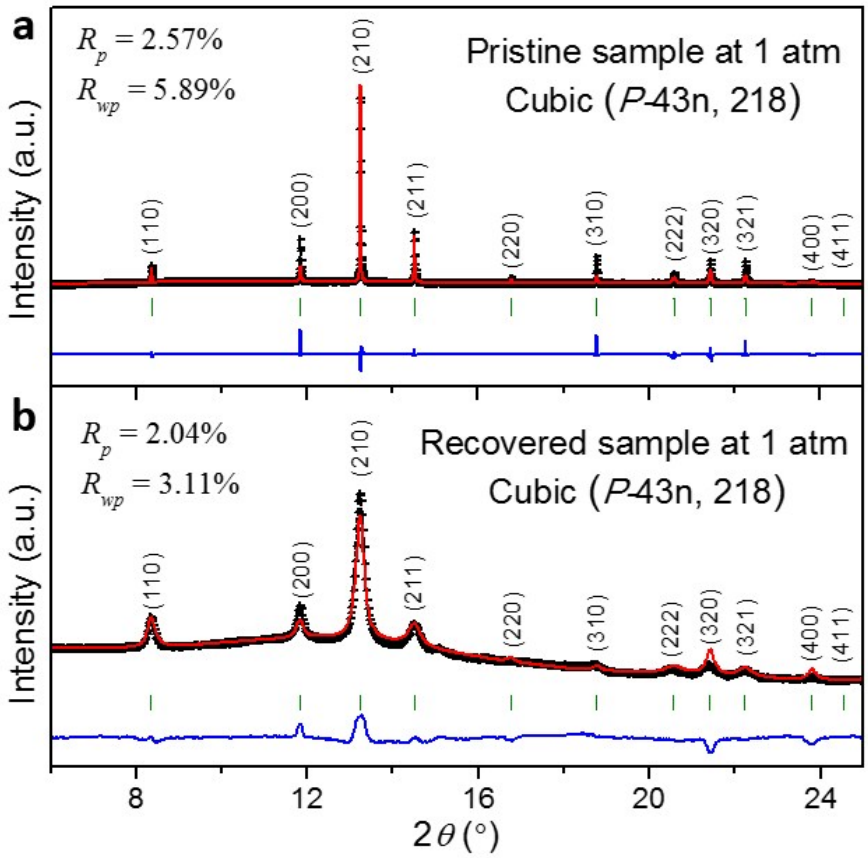

Fig. S6 Comparison between the synchrotron XRD spectra of the pristine sample (at 1 atm) and quenched sample after compression and decompression. (X-ray wavelength is 0.6199 Å)

Refined structural information of Ag_3PO_4 at 9.7 GPa

Table S1. Refined lattice data for Ag_3PO_4 at 9.7 GPa.

Title	Ag_3PO_4
Crystal system	Trigonal
Space group	*R*3c, 161
$a = b$ (Å)	7.67490
c (Å)	11.56120
$\alpha = \beta$	90°
γ	120°
V (Å^3)	589.76502

Table S2. Refined atomic positions and anisotropic displacement parameters for Ag_3PO_4 at 9.7 GPa.

Atom	*x*	*y*	*z*	Wyckoff site	U (Å^2)
Ag	0.68788	0.10834	-0.40531	18b	0.260
O1	0.20838	0.10491	-0.05453	18b	0.035
P	0.66667	0.33333	0.32800	6a	0.192
O4	0.66667	0.33333	-0.56327	6a	0.014

Calculated structural information of Ag_3PO_4 at 10.0 GPa

Table S3. Predicted lattice data for Ag_3PO_4 at 10.0 GPa.

Title	Ag_3PO_4
Crystal system	Trigonal
Space group	*R*3c, 161
$a = b$ (Å)	7.65190
c (Å)	11.72010
$\alpha = \beta$	90°
γ	120°
V (Å^3)	594.29286

Table S4. Predicted atomic positions and anisotropic displacement parameters for Ag_3PO_4 at 10.0 GPa.

Atom	*x*	*y*	*z*	Wyckoff site	U (Å^2)
Ag	0.68447	0.11574	-0.40249	18b	0.013
O1	0.21663	0.06749	-0.05270	18b	0.013
P	0.66667	0.33333	0.32565	6a	0.013
O4	0.66667	0.33333	-0.54339	6a	0.013

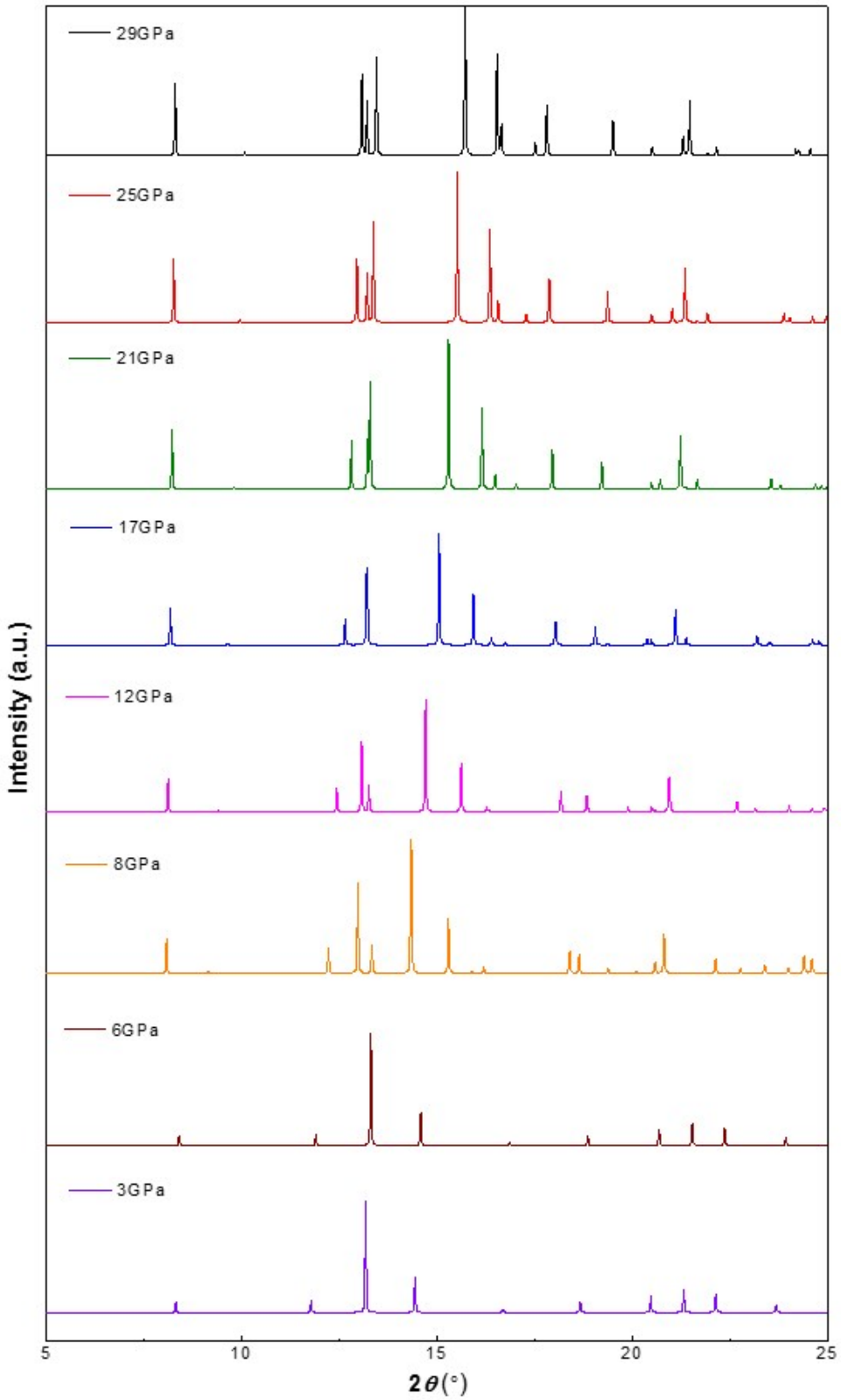

Fig. S7 Theoretical XRD patterns of Ag_3PO_4 under different pressure derived from the predicted crystal structures. (X-ray wavelength is 0.6199 Å)

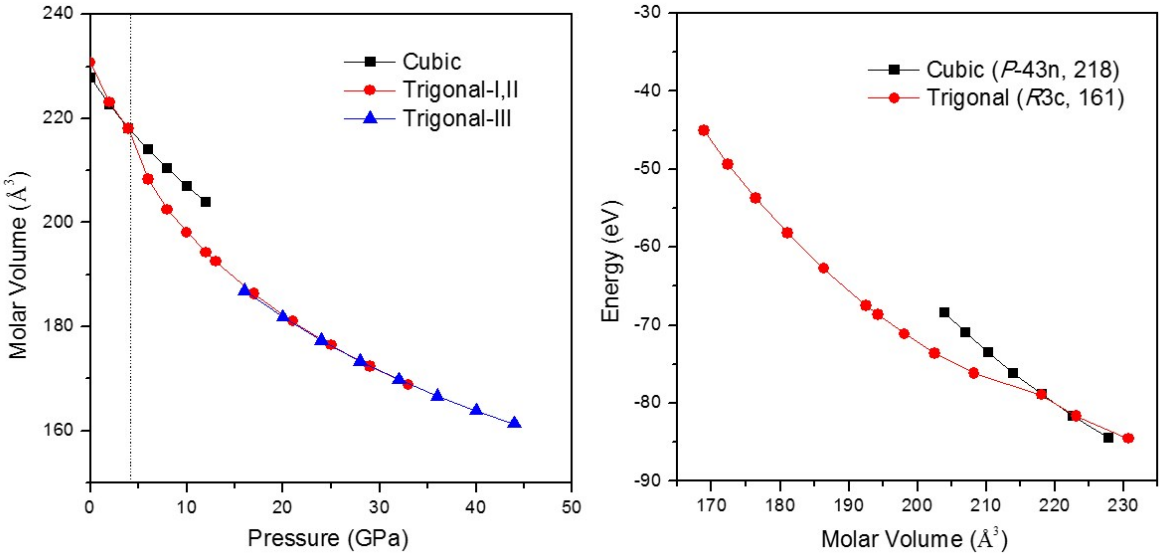

Fig. S8 Calculated volume-pressure plot (left) and energy-volume plot (right) of Ag_3PO_4.

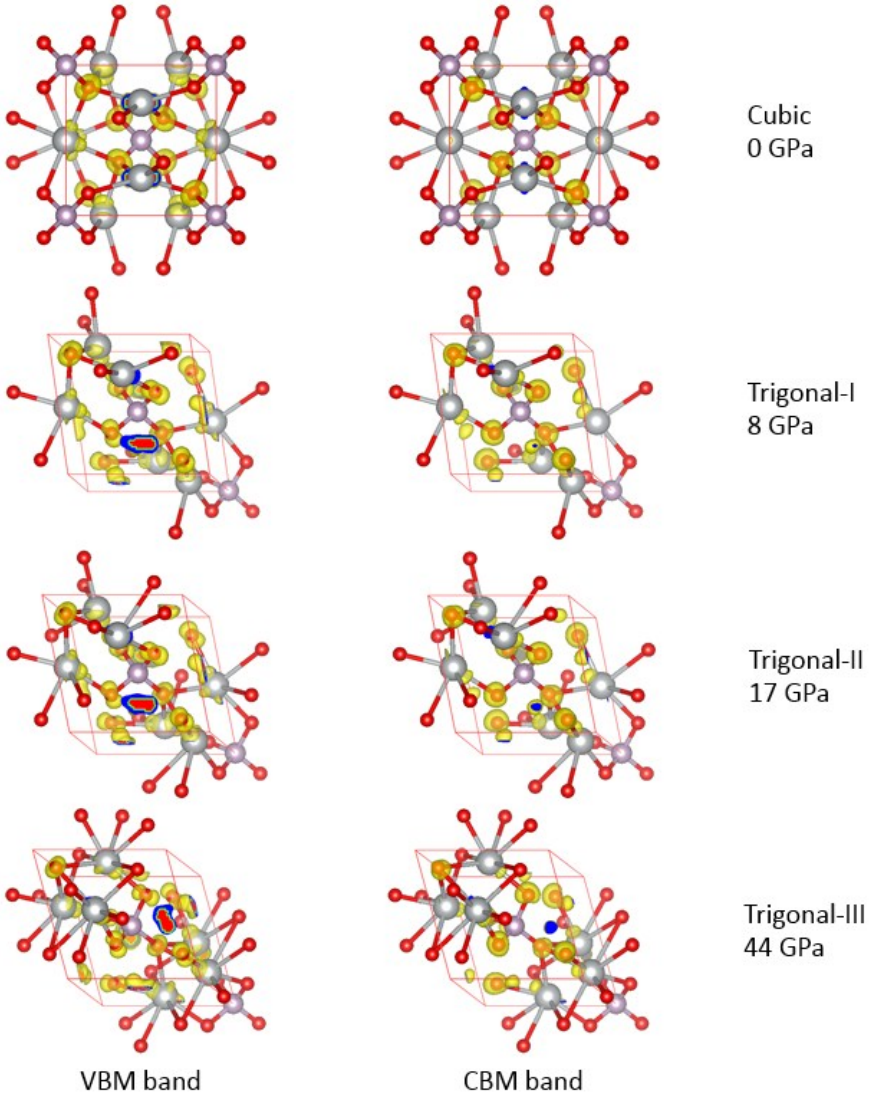

Fig. S9 Partial charge density of VBM and CBM bands for Ag_3PO_4. Grey spheres: Ag atoms; red spheres: O atoms; purple spheres: P atoms.

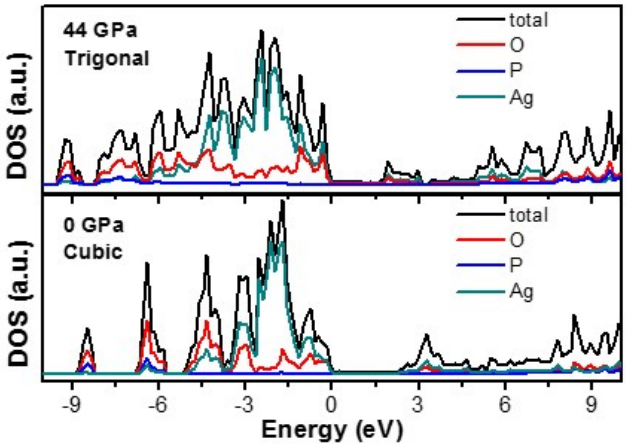

Fig. S10 Total and partial density of states (DOS) of the cubic (0 GPa) and trigonal (44 GPa) Ag_3PO_4.